Available online at www.sciencedirect.com
SCIENCE DIRECT®
Inorganica Chimica Acta 358 (2005) 2283–2291
Inorganica Chimica Acta
www.elsevier.com/locate/ica

Synthesis of a novel pyridine-diamino bridged diphosphine ligand and its macrocyclic metal complexes

Qing-Shan Li *, Chong-Qing Wan, Feng-Bo Xu, Hai-Bin Song, Zheng-Zhi Zhang *

State Key Laboratory of Element-Organic Chemistry, Nankai University, Tianjin 300071, PR China

Received 20 August 2004; accepted 11 January 2005

Abstract

A novel long chain diphosphine ligand with a pyridine-diamino bridge, 2,6-bis(*N*-benzyl-*N*-diphenylphosphinomethylamino)pyridine (PNP1), was prepared conveniently using the Mannich reaction of $HPPh_2$ with paraformaldehyde and 2,6-bis(*N*-benzylamino)pyridine in high yield. Reactions of the ligand with metal complexes, $M(COD)Cl_2$ (M = Pd, Pt), $M(CH_3CN)_4ClO_4$ (M = Cu, Ag) and $M(CO)_6$ (M = Mo, W) afforded the corresponding 10-numbered monometallic macrocyclic complexes with an uncoordinated pyridyl bridge. The monometallic chelate $PdCl_2$(PNP1) continued to react with Ag^+ or Cu^+ giving the μ-Cl bridged bicyclic metallic complex $(\mu\text{-Cl})_2[PdCl(PNP1)]_2$. The diphenylphosphine group coordinated with metal ion in *cis*-form in all the 10-numbered macrocyclic metal complexes. Ligand PNP1 and another known analogous 2,6-bis(*N*-diphenylphosphinoamino)pyridine (PNP2) reacted with $Au(SMe_2)Cl$ giving the corresponding bimetallic Au_2Cl_2(PNP1) and Au_2Cl_2(PNP2), respectively. The latter bimetallic complexes continued to react with Ag^+ and diphosphine ligand to give the corresponding bimetallic macrocyclic complexes $Au_2(ligand)_2(ClO_4)_2$. All the complexes were characterized and the structures of some complexes were confirmed by X-ray single crystallography determination.

Keywords: Diphosphine; P,N-ligand; Macrocyclic metal complexes; Bimetallic complexes; Crystal structures

1. Introduction

Recently, there has been continuing interest in the synthesis and chemistry of hemilabile ligands in view of their wide use in coordination, organometallic and catalytic chemistry, in which the tridentate ligands with PXP (X = C, N, O, S, and As) donor sets [1–3] have attracted particular attention for their coordinative extensibility and structural diversity with transition metals. The functionalized diphosphine ligands with pyridyl as a bridge usually coordinated with metal ions both with N and P atoms, but also some scare cases [2,3] functioned as a diphosphine ligand with an uncoordinated pyridyl group. Thus, the uncoordinated pyridyl groups in diphosphine ligand should have some ability in relation with recognition to metal ions or organic molecules.

The rigid pyridine-diphosphine ligand 2,6-diphosphinopyridine (**A**) was first synthesized by Newkome and Hager [4] and its coordination with metal species to form various binuclear and polynuclear metal complexes was extensively studied [5]. The rigidity of ligand **A** governs the P–N–P ligand bite distance and the two P donors could not bind to a single metal atom. Therefore, ligand A could coordinate to metal in several bridging modes as shown in Scheme 1(a)–(d): (a) two P atoms coordinate to two metal atoms with a pyridyl-N atom

* Corresponding author. Tel.: +86 22 2350 4235; fax: +86 22 2350 3438.
E-mail addresses: qli@nankai.edu.cn, qingshanli2004@yahoo.com.cn (Q.-S. Li).

0020-1693/$ - see front matter © 2005 Published by Elsevier B.V.
doi:10.1016/j.ica.2005.01.008

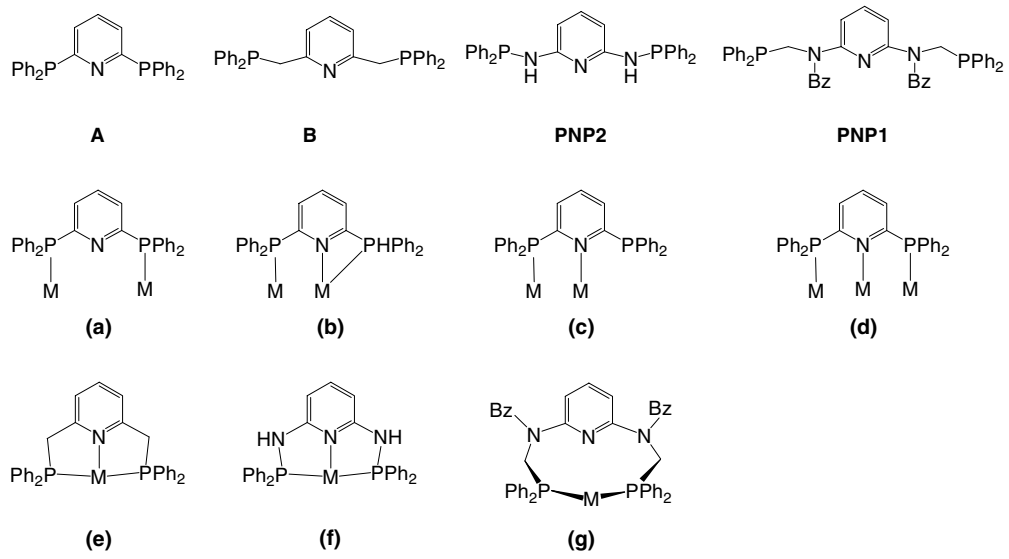

Scheme 1.

uncoordinated; (b) a P atom and the pyridyl-N atom chelate to one metal and the other P atom coordinates with a second metal atom; (c) one P and the pyridyl-N atom bond to two metal atoms, respectively, with the other P atom uncoordinated, (d) each atom of the three donors bonds to a separate metal atom. The pyridyl bridged longer chain diphosphine, 2,6-bis(diphenylphosphinomethyl)pyridine (**B**), which was more flexible, could coordinate to metal with three donor atom bonding to a single metal [6], its complexes had a favorite configuration of two abutted five-member cycle as shown in Scheme 1(e). An analog of ligand **B**, 2,6-bis(diphenylphosphinoamino)pyridine (PNP2) [7], bridged with a similar chain in length, but with two NH groups instead of two CH_2 in **B**, was first studied in coordination chemistry by Haupt and co-workers in 1987. Less metal complexes of PNP2 were observed in the literature [7] because of its lower flexibility compared with those of ligand **B** and the metal complexes had the structure of bi-five-member cycle configuration as shown in Scheme 1(f). For the attempt to synthesize the macrocyclic metal complexes and to study on their unique catalytic properties, herein a much longer pyridyl chain bridged diphosphine was prepared and its coordinated macrocyclic metal complexes with structure as shown in Scheme 1(g) were studied.

2. Results and discussion

2.1. Preparation of ligand PNP1 and its 10-numbered macrocyclic metal complexes and the X-ray structure determination

The ligand PNP1 was synthesized conveniently using the Mannich reaction of $HPPh_2$ with paraformaldehyde and 2,6-bis(*N*-benzylamino)pyridine in high yield. PNP1 reacted with metal complexes $M(COD)Cl_2$ (M = Pd, Pt), $M(CH_3CN)_4ClO_4$ (M = Cu, Ag) and $M(CO)_6$ (M = Mo, W) to afford the corresponding 10-numbered monometallic macrocyclic complexes (**1**–**6**) with an uncoordinated pyridyl bridge (Scheme 2). The monometallic chelate $PdCl_2$(PNP1) (**1**) continued to react with Ag^+ or Cu^+ giving the μ-Cl bridged bicyclic metallic complex $[Pd(PNP1)]_2(\mu\text{-}Cl)_2(ClO_4)_2$ (**7**).

The two arms in ligand PNP1 are longer than its analog 2,6-bis(diphenylphosphinoamino)pyridine (PNP2). For ligand PNP2, the two P atoms and one N atom in pyridyl could bond to a same metal atom (such as Mo, W, Pd, Ni and Pt) [7] to form the abutted bis-penta-cycle structure of monometallic complexes [Scheme 1(f)]. But for ligand PNP1, when the two P atoms chelate to one metal, the N atom in pyridyl could not bond to the same metal due to the tension of bis-hexa-cycle

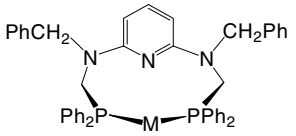

M = $PdCl_2$, **1**; $PtCl_2$, **2**; $Cu(NCCH_3)_2ClO_4$, **3**; $Ag(NCCH_3)_2ClO_4$, **4**; $Mo(CO)_4$, **5**; $W(CO)_4$, **6**

Scheme 2.

with three N atoms and one metal atom in one plane. Therefore, all the monometallic complexes of ligand PNP1 take the structure with two P atoms chelating to metal atom and the pyridine-N atom uncoordinated (Scheme 2). The structures of these complexes adopt an *endo*-configuration to form a boat shape of the molecule and the two P atoms are all in *cis*-form, which is confirmed by the X-ray crystal structure determination of some complexes (Figs. 2–5).

The structures of ligand PNP1 and complexes **1**, **3**, **5**, **7** are shown in Figs. 1–5, while the important bond distances and angles are listed in Table 2. In complex **1**, the Pd atom adopted a planar square configuration with a *cis*-form of two P and two Cl atoms. The P–Pd bond distance of 2.2517(14) Å is very compatible to those reported in the literature, but longer than those of 2.212(2) Å for *cis*-$Re_2(m\text{-}O_2C_6H_4\text{-}4\text{-}PPh_2)_2Cl_2(dppm)_2$ (Pd_2Cl_4) [8] and 2.1969(15) Å for [$PdCl_2(Ph_2PCH_2CH(Ph)NHPh)$] [9]. The distance of Pd(1) to N(2) is 3.175(4) Å. The angles of P(1)–Pd(1)–P(2), P(2)–Pd(1)–Cl(1) and Cl(2)–Pd(1)–Cl(1) are 96.16(5), 83.72(5) and 91.39(5), respectively, making the Pd plane slightly distorted. Positions of the two benzyls and the two methylenes changed from *trans*- to *cis*-form of the pyridyl plane compared with those in free ligand PNP1. The whole

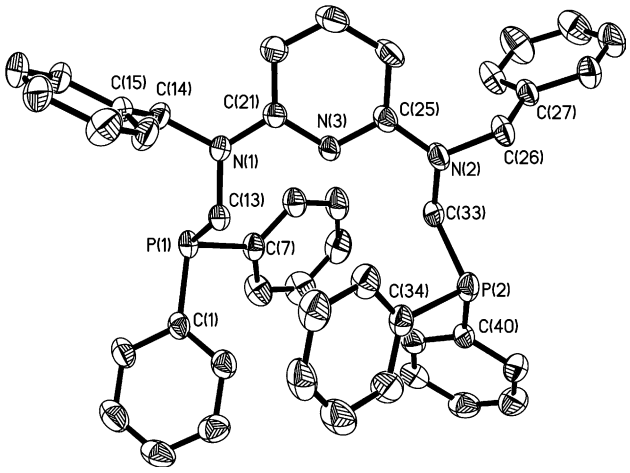

Fig. 1. Perspective drawing of ligand PNP1. Thermal ellipsoids are shown at the 30% probability level.

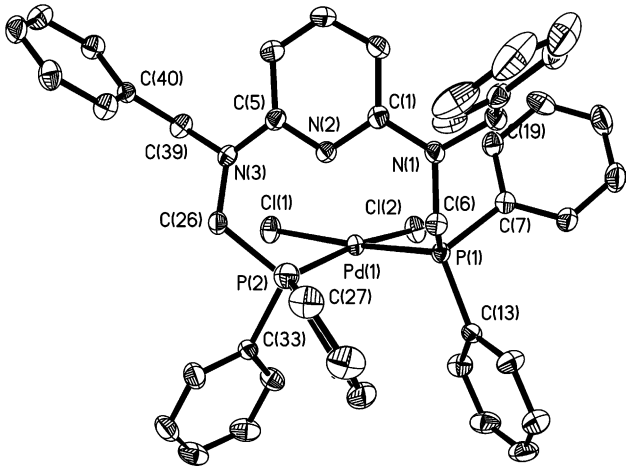

Fig. 2. Perspective drawing of complex $\mathbf{1}\cdot CH_2Cl_2$ with solvent molecule omitted for clarity. Thermal ellipsoids are shown at the 30% probability level.

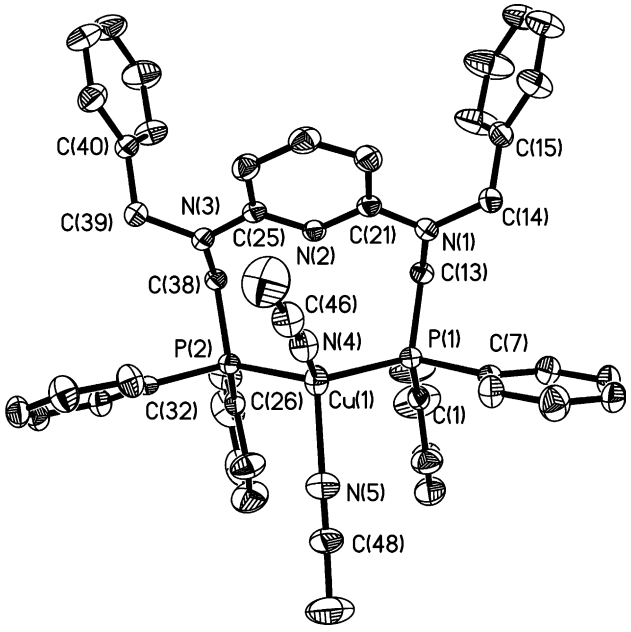

Fig. 3. Perspective drawing of the cation part in complex **3** with ClO_4^- omitted for clarity. Thermal ellipsoids are shown at the 30% probability level.

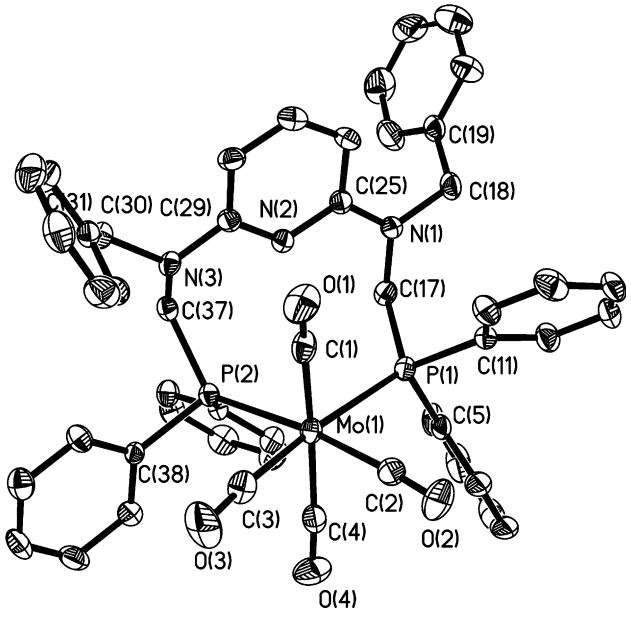

Fig. 4. Perspective drawing of complex **5**. Thermal ellipsoids are shown at the 30% probability level.

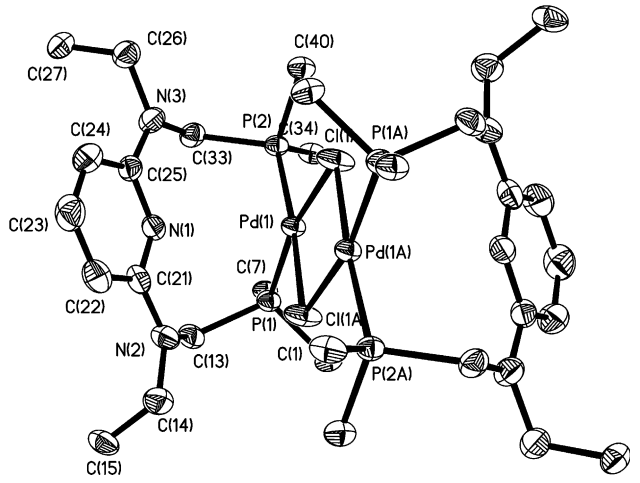

Fig. 5. Perspective drawing of the cation part in complex $7 \cdot 1.5CH_2ClCH_2Cl$ with solvent, ClO_4^- and phenyl ring omitted for clarity. Thermal ellipsoids are shown at the 30% probability level.

molecule structure adopts a boat fashion to form a 10-membered macrocycle (Fig. 3).

Complexes of Cu(I) and Ag(I) were obtained by the same procedure as those of Pt and Pd, except that preparation and manipulation of complex **4** in dark environment because of photosensitivity of Ag complex. In **3**, the Cu atom adopted a tetrahedron configuration with two P atoms and two CH_3CN coordinated. The P–Cu bond distance of 2.2608(12) Å is similar to those reported in the literature, such as those of 2.23–2.27 Å for $[Cu(NN')_2(DPEphos)]BF_4$ (DPEphos = bis[2-(diphenylphosphino)phenyl]ether and NN′ = bidentate N-ligand) [10]. The angles of N(4)–Cu(1)–N(5), P(1)–Cu(1)–P(2) and N(4)–Cu(1)–P(1) are 98.42(17)°, 113.66(4)° and 117.51(11)°, respectively. Complex **3** had a space group of $P\bar{1}$, and also adopted a boat shape configuration, with a symmetric mirror existing through the plane of N(2)–N(4)–N(5)–Cu(1) (Fig. 4).

Complexes **5** and **6** were prepared by the thermal reaction of PNP1 with $Mo(CO)_6$ and $W(CO)_6$, respectively. In **5**, the center Mo atom adopted an octahedron configuration with two *cis*-P atoms and four carbonyls. The full molecule took a distorted boat fashion. The angle of P(1)–C(17)–N(1) is 114.9(4)°, which is lesser than that of P(2)–C(37)–N(3) [117.3(3)°]. The P–Mo bond distances in **5** of 2.5752(15) and 2.5942(16) Å are similar to $Mo_2Cl_4(\mu\text{-}L)_2$ (L = 2-chloro-6-(diphenylphosphino) pyridine) of 2.550(5) Å [11] (Fig. 5).

Complex **1** reacted with Ag^+ or Cu^+ to afford complex **7**. In **7**, the two subunits of formule adopted *trans*-fashion. The two pyridyl rings in *trans*-form were parallel to each other and deposited on the two sides of the bridge plane. The corresponding bond distances and bond angles in **7** were extraordinarily compatible with those in **1**.

In ^1H NMR spectra of these macrocyclic monometallic complexes, the signal of CH_2 group linked with PPh_2 was shifted downfield to 4.65–4.97 ppm compared with that in free ligand PNP1 of 4.34 ppm. The signals of PPh_2 were also shifted downfield. However, the other CH_2 in benzyl group showed a high-field shift to about 3.44–4.26 ppm from 4.50 ppm in free ligand, especially to 3.44 ppm in complex **5**. The electronic absorptions of all complexes in dichloromethane showed a strong absorption band at ca. 262 nm and a weak band at ca. 334 nm, which underwent a slight red shift in the UV–Vis spectrum compared with the corresponding band of free PNP1 at 254 and 326 nm. All these phenomena were consistent with the coordination of phosphine ligand with transition metal.

2.2. Preparation of Au–Au bond containing bicyclic complexes of pyridine-bridged diphosphine

The macrocyclic bimetallic complexes of Au–Au bond were synthesized as shown in Scheme 3. First, ligands PNP1 and PNP2 reacted with $Au(SMe_2)Cl$ giving the corresponding bimetallic Au_2Cl_2(PNP1) (**8**) and Au_2Cl_2(PNP2) (**10**), respectively, with a simple strategy used to generate R_3PAuCl (R = aryl or alkyl) in the literature [12,13]. Then, the latter bimetallic complexes continued to react with Ag^+ and another diphosphine ligand to give the corresponding bimetallic macrocyclic complexes $Au_2(\mu\text{-}L)_2(ClO_4)_2$ (**9** and **11**) (Scheme 3). The molecular structure of complex **8** is shown in Fig. 6 and the selected bond distances and bond angles

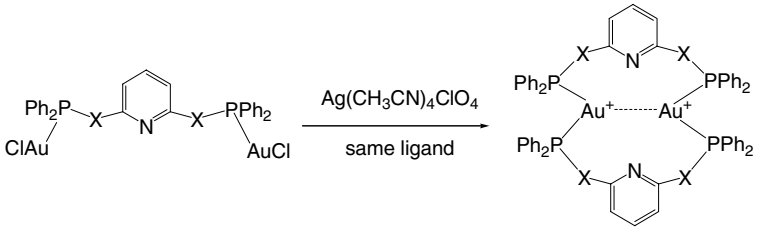

X = NH, **8**

X = N(CH$_2$Ph)CH$_2$, **10**

X = NH, **9**

X = N(CH$_2$Ph)CH$_2$, **11**

Scheme 3.

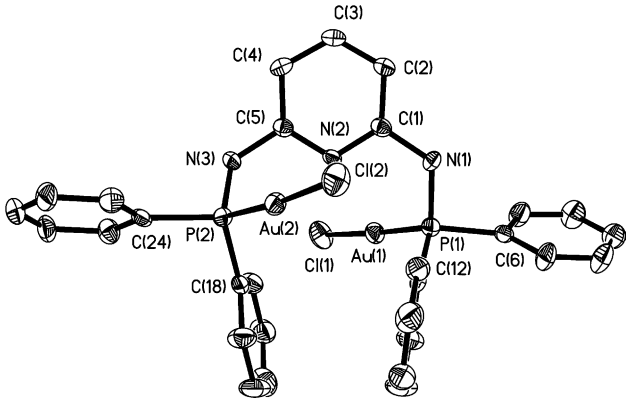

Fig. 6. Perspective drawing of complex **8** with solvent omitted for clarity. Thermal ellipsoids are shown at the 30% probability level.

in Table 2. The space group of crystal molecule of **8** is $P\bar{1}$. Because of the single crystal suit for X-ray determination grown by recrystallization in a mixture solvent of DMSO, CH_3COCH_3 and Et_2O, there are two molecules of DMSO solvent existing in one molecular of **7** in the crystal structure. The bond lengths of Au–P and Au–Cl are 2.222(2) and 2.293(3) Å, respectively, and the bond angles of P(1)–Au(1)–Cl(1) and P(2)–Au(2)–Cl(2) are 177.54(10)° and 175.25(9)°, respectively. The main bond distances and angles were consistent with those in the literature [12,13].

3. Experimental

Ligands PNP2 [7] and 2,6-bis(*N*-benzylamino)pyridine were prepared as reported in the literature. All other reagents and organic solvents were purchased from commercial sources. All reactions were carried out under a prepurified nitrogen atmosphere using standard Schlenk techniques on vacuum line. All solvents were thoroughly dried and deoxygenated by standard methods and distilled immediately before use. ^{1}H and ^{31}P NMR spectra were recorded on a Bruker AC-300 NMR spectrometer. IR spectra were recorded on a Bruker FT-IR Equinox-55 infrared spectrophotometer in the range of 4000–400 cm^{-1} using KBr disks. The UV spectra were conducted on a Shimadzu UV-1601PC spectrophotometer. Elemental analyses were performed on a Yanaco MT-3 analyzer. Melting points were determined on a Yanaco micromelting point apparatus MP-500.

3.1. Preparation of PNP1

2,6-Bis(*N*-diphenylphosphinomethyl-*N*-benzyl) aminopyridine (PNP1) was prepared by the Mannich reaction of $HPPh_2$. $HPPh_2$ (7.44 g, 40 mmol) was added with stirring to a solution of 2,6-bis(*N*-benzylamino)pyridine (5.78 g, 20 mmol) and paraformaldehyde (1.5 g, 30 mmol) in toluene (50 mL) at 70–80 °C. The mixture was stirred at 70–80 °C until all of paraformaldehyde had completely disappeared (about 24 h). The solution was cooled and then filtered through Celite. The solvent was removed under vacuum and the residue was recrystallized with CH_2Cl_2/CH_3OH to give 5.70 g (41.6%) of PNP1 as a white powder. m.p. 112–114 °C. The sample for analysis was further purified by recrystallization from CH_2Cl_2/*n*-hexane. *Anal*. Calc. for $C_{45}H_{41}N_3P_2$: C, 78.81; H, 6.03; N, 6.13. Found: C, 78.73; H, 6.08; N, 6.19%. ^{1}H NMR ($CDCl_3$, δ, ppm): 7.02–7.41 (m, 31H, 6Ph and Py-H^4), 5.86 (d, 2H, Py-H^3/H^5), 4.50 (s, 4H, 2CH_2Ph), 4.34 (d, 4H, 2CH_2PPh$_2$). ^{31}P NMR ($CDCl_3$, δ, ppm): −23.5.

3.2. Preparation of $PdCl_2$(PNP1) · CH_2Cl_2 (**1** · CH_2Cl_2)

The solid of Pd(COD)Cl_2 (0.171 g, 0.60 mmol) was added to the solution of PNP1 (0.411 g, 0.6 mmol) in CH_2Cl_2 (30 ml) and the mixture was stirred for 0.5 h at room temperature. The solvent was removed under vacuum and the residue was recrystallized with CH_2Cl_2/Et_2O to give 0.482 g (82%) of **1** as a yellow powder. m.p. 224–226 °C. The sample for analysis was further purified by recrystallization from CH_2Cl_2/*n*-hexane and was found to be formule of $PdCl_2$(PNP1) · CH_2Cl_2. *Anal*. Calc. for $C_{46}H_{43}Cl_4PdN_3P_2$: C, 58.28; H, 4.57; N, 4.43. Found: C, 58.19; H, 4.55; N, 4.46%. ^{1}H NMR ($CDCl_3$, δ, ppm): 7.53–7.05 (m, 31H, 6Ph and Py-H^4), 5.88 (d, 2H, Py-H^3/H^5), 4.97(d, 4H, 2CH_2PPh$_2$), 4.18 (s, 4H, 2CH_2Ph), ^{31}P NMR ($CDCl_3$, δ, ppm): 21.27(s).

3.3. Preparation of $PtCl_2$(PNP1) · CH_2Cl_2 (**2** · CH_2Cl_2)

The same procedure as that for **1** was followed, but Pt(COD)Cl_2 (0.112 g, 0.3 mmol) and PNP1 (0.2055 g, 0.6 mmol) were used to afford 0.268 g (84%) of **2** as a bright yellow powder. m.p. 256–260, *Anal*. Calc. for $C_{46}H_{43}Cl_4PtN_3P_2$: C, 53.29; H, 4.18; N, 4.05. Found: C, 53.25; H, 4.26; N, 4.07%. ^{1}H NMR ($CDCl_3$, δ, ppm): 7.54–7.07 (m, 31H, 6Ph and Py-H^4), 5.90 (d, 2H, Py-H^3/H^5), 4.83 (d, 4H, 2CH_2PPh$_2$), 4.17 (s, 4H, CH_2Ph), ^{31}P NMR ($CDCl_3$, δ, ppm): 2.99 (t, J_{Pt-P} = 3880 ppm).

3.4. Preparation of $Cu(CH_3CN)_2$(PNP1)ClO_4 (**3**)

Similarly, $Cu(CH_3CN)_4ClO_4$ (0.096 g, 0.3 mmol) and PNP1 (0.205 g, 0.6 mmol) were used to afford 0.244 g (81%) of **3** as a white powder. m.p. 196–200 °C. *Anal*. Calc. for $C_{49}H_{47}ClCuN_5P_2O_4$: C, 63.22; H, 5.09; N, 7.52. Found: C, 63.00; H, 4.97; N, 7.60%. ^{1}H NMR ($CDCl_3$, δ, ppm): 7.53–6.98 (m, 31H, 6Ph and Py-H^4), 5.81 (d, 2H, Py-H^3/H^5), 4.73 (d, 4H, 2CH_2PPh$_2$), 4.26

(s, 4H, 2CH_2Ph), 4.07(s, 6H, 2CH_3CN), ^{31}P NMR ($CDCl_3$, δ, ppm): −10.10.

3.5. Preparation of $Ag(CH_3CN)_2(PNP1)ClO_4$ (4)

Similarly, $Ag(CH_3CN)_4ClO_4$ (0.111 g, 0.3 mmol) and PNP1 (0.205 g, 0.6 mmol) were used to afford 0.268 g (84%) of **4** as a white powder. m.p. 158–160 °C. *Anal.* Calc. for $C_{49}H_{47}ClAgN_5P_2O_4$: C, 60.35; H, 4.86; N, 7.18. Found: C: 60.93; H, 4.83; N, 6.98%. ^{1}H NMR ($CDCl_3$, δ, ppm): 7.53–7.92 (m, 31H, 6Ph and Py-H^4), 5.89 (d, 2H, Py-H^3/H^5), 4.67(d, 4H, 2CH_2PPh$_2$), 4.16 (s, 4H, 2CH_2Ph), 3.97(s, 6H, 2CH_3CN), ^{31}P NMR ($CDCl_3$, δ, ppm): −11.61 [J(P–^{107}Ag) = 478.0, J(P–^{109}Ag) = 586.4 ppm].

3.6. Preparation of $Mo(CO)_4(PNP1)$ (5)

The same procedure as that for **1** was followed, but $Mo(CO)_6$ (0.132 g, 50 mmol) and PNP1 (0.348 g, 50 mmol) were reacted in CH_3CN (10 ml) to reflux for 3 h, 0.307 g (62%) of **5** was obtained as a gray powder. m.p. 174–176 °C. *Anal.* Calc. for $C_{49}H_{41}MoN_3O_4P_2$: C, 65.85; H, 4.62; N, 4.70. Found: C, 65.79; H, 4.58; N, 4.69%. IR (KBr disk, cm^{-1}): ν 1859–2017 (ν(CO)). ^{1}H NMR ($CDCl_3$, δ, ppm): 7.51–7.11 (m, 31H, 6Ph and Py-H^4), 5.71 (d, 2H, Py-H^3/H^5), 4.65 (s, 4H, 2CH_2PPh$_2$), 3.44 (d, 4H, 2CH_2Ph), ^{31}P NMR ($CDCl_3$, δ, ppm): 16.62.

3.7. Preparation of $W(CO)_4(PNP1)$ (6)

Similarly, $W(CO)_6$ (0.141 g, 0.4 mmol) and PNP1 (0.274 g, 0.4 mmol) were reacted in THF (20 ml) to reflex for 10 h, 0.230 g (55.6%) of **6** was obtained as a yellow powder. m.p. 112–114 °C. *Anal.* Calc. for $C_{49}H_{41}WN_3O_4P_2$: C, 59.95; H, 4.21; N, 4.28. Found: C, 59.89; H, 4.17; N, 4.27%. IR: (KBr disk, cm^{-1}): ν 1864–2016 (ν(CO)). ^{1}H NMR ($CDCl_3$, δ, ppm): 7.60–7.00 (m, 31H, 6Ph and Py-H^4), 5.89 (d, 2H, Py-H^3/H^5), 4.78 (s, 4H, 2CH_2PPh$_2$), 3.54 (d, 4H, 2CH_2Ph), ^{31}P NMR ($CDCl_3$, δ, ppm): 25.5.

3.8. Preparation of $[Pd(PNP1)]_2(\mu\text{-}Cl)_2(ClO_4)_2 \cdot 1.5CH_2ClCH_2Cl$ ($7 \cdot 1.5CH_2ClCH_2Cl$)

Similarly, $Cu(CH_3CN)_4ClO_4$ (0.065 g, 0.2 mmol) and **1** (0.190 g, 0.2 mmol) were reacted in CH_2Cl_2 (30 ml) for 1 h, 0.200 g (87%) of **7** was obtained as a yellow powder. m.p. 140–142 °C. The crystal sample for analysis was further purified by recrystallization from CH_2ClCH_2Cl/cyclohexane. Analysis and subsequent refinement of the X-ray structure of a crystal of **7** showed that it had the composition of $C_{90}H_{82}Cl_2N_6P_4Pd_2(ClO_4)_2 \cdot 2CH_2ClCH_2Cl$. *Anal.* Calc. for $C_{93}H_{88}Cl_7N_6O_8P_4Pd_2$: C, 55.78; H, 4.43; N, 4.20. Found: C, 56.10; H, 4.01; N, 4.36%. ^{1}H NMR ($CDCl_3$, δ, ppm): 7.05–7.55 (m, 62H, 12Ph and 2Py-H^4), 5.70 (d, 4H, 2Py-H^3/H^5), 3.99 (s, 8H, 4CH_2Ph), 4.49 (d, 8H, 4CH_2PPh$_2$), ^{31}P NMR ($CDCl_3$, δ, ppm): 25.00.

3.9. Preparation of $Au_2Cl_2(PNP2)$ (8)

Similarly, $Au(SMe_2)Cl$ (0.236 g, 0.8 mmol) and PNP2 (0.195 g, 0.4 mmol) were stirred in CH_2Cl_2 (30 ml) for 0.5 h at room temperature to afford 0.355 g (82%) of **8** as a white powder. m.p. 232–234 °C. *Anal.* Calc. for $C_{29}H_{25}Au_2Cl_2N_3P_2$: C, 36.96; H, 2.67; N, 4.46. Found: C, 37.11; H, 2.31; N, 4.65%. ^{1}H NMR ($CDCl_3$, δ, ppm): 7.22–7.34 (m, 21H, 4Ph and Py-H^4), 6.34 (d, 2H, Py-H^3/H^5). ^{31}P NMR ($CDCl_3$, δ, ppm): 52.34.

3.10. Preparation of $Au_2(PNP2)_2(ClO_4)_2$ (9)

Similarly, **8** (0.188 g, 0.2 mmol) and $Ag(CH_3CN)_4ClO_4$ (0.148 g, 0.4 mmol) were reacted in CH_2Cl_2 (30 ml) for 0.5 h at room temperature. Then, ligand PNP2 (0.098 g, 0.2 mmol) was added and the mixture was continued to react for 1 h, 0.210 g (82%) of **9** was obtained as a white powder. m.p. 206–208 °C. *Anal.* Calc. for $C_{58}H_{50}Au_2Cl_2N_6O_8P_4$: C, 45.01; H, 3.26; N, 5.43. Found: C, 44.97; H, 3.51; N, 5.61%. ^{1}H NMR ($CDCl_3$, δ, ppm): 7.12–7.44 (m, 42H, 8Ph and 2Py-H^4), 6.55 (d, 4H, 2Py-H^3/H^5). ^{31}P NMR ($CDCl_3$, δ, ppm): 65.59.

3.11. Preparation of $Au_2Cl_2(PNP1)$ (10)

Similarly, $Au(SMe_2)Cl$ (0.059 g, 0.2 mmol) and PNP1 (0.068 g, 0.1 mmol) were reacted in CH_2Cl_2 (30 ml) to give 0.071 g (56%) of **10** as a white powder. m.p. 160–162 °C. *Anal.* Calc. for $C_{45}H_{41}Cl_2Au_2N_3P_2$: C, 46.97; H, 3.59; N, 3.65. Found: C, 47.10; H, 3.51; N, 3.74%. ^{1}H NMR ($CDCl_3$, δ, ppm): 7.62–7.10 (m, 31H, 6Ph and Py-H^4), 5.88 (d, 2H, Py-H^3/H^5), 5.19 (s, 4H, 2CH_2PPh$_2$), 4.16 (d, 4H, 2CH_2Ph), ^{31}P NMR ($CDCl_3$, δ, ppm): 19.96.

3.12. Preparation of $Au_2(PNP1)_2(ClO_4)_2$ (11)

Similarly, **10** (0.115 g, 0.1 mmol) and $Ag(CH_3CN)_4ClO_4$ (0.074 g, 0.2 mmol) were reacted in CH_2Cl_2 (30 ml) for 0.5 h at room temperature. Then, ligand PNP1 (0.068 g, 0.1 mmol) was added and the mixture was continued to react for 1 h, 0.130 g (86%) of **11** was obtained as a green powder. m.p. 160–164 °C. *Anal.* Calc for $C_{90}H_{82}Cl_2Au_2N_6O_8P_4$: C, 55.02; H, 4.21; N, 4.28. Found: C, 55.09; H, 4.22; N, 4.10%. ^{1}H NMR ($CDCl_3$, δ, ppm): 7.53–6.93 (m, 62H, 12Ph and 2Py-H^4), 5.86 (d, 4H, 2Py-H^3/H^5), 4.30 (s, 8H, 4CH_2PPh$_2$), 3.47 (d, 8H, CH_2Ph), ^{31}P NMR ($CDCl_3$, δ, ppm): 34.45.

Table 1
Crystal data and refinement parameters

	PNP1	**1** · CH_2Cl_2	**3**	**5**	**7** · 1.5CH_2ClCH_2Cl	**8** · 2DMSO
Formula	$C_{45}H_{41}N_3P_2$	$C_{46}H_{43}Cl_4N_3P_2Pd$	$C_{49}H_{47}ClCuN_5O_4P_2$	$C_{49}H_{41}MoN_3O_4P_2$	$C_{93}H_{88}Cl_7N_6O_8P_4Pd_2$	$C_{33}H_{37}Au_2Cl_2N_3O_2P_2S_2$
Formula weight	685.75	947.97	930.85	893.73	2002.52	1096.53
Crystal system	triclinic	monoclinic	triclinic	monoclinic	monoclinic	triclinic
Space group	$P\bar{1}$	$P2_1/n$	$P\bar{1}$	$P2_1/c$	$P2_1/n$	$P\bar{1}$
a (Å)	8.854(5)	13.785(4)	10.457(3)	18.889(6)	12.926(4)	11.852(5)
b (Å)	11.231(6)	17.298(5)	11.483(3)	10.183(3)	17.962(5)	12.840(5)
c (Å)	18.955(11)	18.139(5)	20.210(6)	22.019(7)	20.793(6)	13.476(5)
α (°)	91.231(9)	90	98.813(4)	90	90	92.762(7)
β (°)	91.336(9)	92.825(5)	92.920(5)	91.168(6)	107.186(5)	106.749(6)
γ (°)	90.954(10)	90	104.144(5)	90	90	96.649(7)
V (Å^3)	1883.6(18)	4320(2)	2315.4(11)	4234(2)	4612(2)	1943.4(13)
Z	2	4	2	4	2	2
D_{calcd} (g cm^{-3})	1.209	1.458	1.335	1.402	1.442	1.874
μ (mm^{-1})	0.151	0.788	0.648	0.434	0.720	7.900
F(0 0 0)	724	1936	968	1840	2046	1048
Crystal size (mm)	0.22 × 0.20 × 0.16	0.18 × 0.16 × 0.08	0.26 × 0.22 × 0.20	0.18 × 0.16 × 0.14	0.30 × 0.22 × 0.12	0.20 × 0.18 × 0.18
λ (Å)	0.71073	0.71073	0.71073	0.71073	0.71073	0.71073
θ_{min}–θ_{max} (°)	1.07–26.40	1.63–26.42	1.02–26.46	1.08–25.01	1.66–26.47	1.58–25.01
T (K)	293(2)	293(2)	293(2)	293(2)	293(2)	293(2)
Number of data collected	10 352	24 672	13 528	21 383	26 469	10 125
Number of unique data	7434	8832	9407	7459	9500	6814
R_{int}	0.0327	0.0863	0.0224	0.1040	0.0650	0.0298
Number of refined parameters	451	505	607	532	586	451
Goodness-of-fit on F^2[a]	1.070	1.009	1.017	0.981	1.046	1.012
Final R indices[b]						
R_1	0.0674	0.0530	0.0592	0.0562	0.0636	0.0392
wR_2	0.1585	0.0995	0.1380	0.0977	0.1481	0.0815
R indices (all data)						
R_1	0.1327	0.1221	0.1013	0.1363	0.1328	0.0772
wR_2	0.1884	0.1267	0.1636	0.1274	0.1841	0.0977
Final difference map (e Å^{-3})	0.299, −0.304	0.506, −0.463	1.638, −1.083	0.409, −0.424	1.006, −0.546	1.060, −1.287
Refinement method	full-matrix least-squares on F^2					

[a] Goodness-of-fit = $[\sum \omega(F_o^2 - F_c^2)^2/(n-p)]^{1/2}$, where n is the number of reflections and p is the number of parameters refined.
[b] $R_1 = \sum(||F_o| - |F_c||)/\sum|F_o|$; $wR_2 = 1/[\sigma^2(F_o^2) + (0.0691P) + 104100P]$, where $P = (F_o^2 + 2F_c^2)/3$.

Table 2
Selected bond distances (Å) and angles (°) with estimated standard deviations

Ligand PNP1			
P(1)–C(13)	1.860(4)	N(1)–C(13)	1.452(4)
P(2)–C(33)	1.864(3)	N(2)–C(33)	1.447(4)
C(21)–N(1)–C(13)	121.9(3)	C(25)–N(2)–C(33)	121.4(3)
N(1)–C(13)–P(1)	114.2(2)	N(2)–C(33)–P(2)	114.3(2)
Complex ***1***			
Pd(1)–P(1)	2.2517(14)	P(1)–C(6)	1.868(5)
Pd(1)–P(2)	2.2610(15)	P(2)–C(26)	1.852(5)
Pd(1)–Cl(2)	2.3442(15)	N(1)–C(6)	1.445(6)
Pd(1)–Cl(1)	2.3584(15)	N(3)–C(26)	1.454(6)
P(1)–Pd(1)–P(2)	96.16(5)	P(1)–Pd(1)–Cl(1)	175.25(5)
P(1)–Pd(1)–Cl(2)	89.57(5)	P(2)–Pd(1)–Cl(1)	83.72(5)
P(2)–Pd(1)–Cl(2)	168.62(5)	Cl(2)–Pd(1)–Cl(1)	91.39(5)
Complex ***3***			
Cu(1)–N(4)	2.017(4)	P(1)–C(13)	1.856(4)
Cu(1)–N(5)	2.155(4)	P(2)–C(38)	1.858(3)
Cu(1)–P(1)	2.2608(12) 0	N(1)–C(13)	1.455(5)
Cu(1)–P(2)	2.2620(12)	N(3)–C(38)	1.452(5)
N(4)–Cu(1)–N(5)	98.42(17)	N(5)–Cu(1)–P(2)	108.29(13)
N(4)–Cu(1)–P(1)	117.51(11)	P(1)–Cu(1)–P(2)	113.66(4)
N(5)–Cu(1)–P(1)	104.39(12)	C(21)–N(1)–C(13)	119.7(3)
N(4)–Cu(1)–P(2)	112.59(11)	C(25)–N(3)–C(38)	119.9(3)
Complex ***5***			
Mo(1)–P(2)	2.5752(15)	P(2)–C(37)	1.862(5)
Mo(1)–P(1)	2.5942(16)	N(1)–C(17)	1.436(6)
P(1)–C(17)	1.885(5)	N(3)–C(37)	1.456(6)
P(2)–Mo(1)–P(1)	96.41(5)	C(37)–P(2)–Mo(1)	124.81(17)
C(3)–Mo(1)–P(2)	88.66(17)	C(25)–N(1)–C(17)	120.8(5)
C(2)–Mo(1)–P(2)	173.73(18)	C(29)–N(3)–C(37)	117.3(4)
C(3)–Mo(1)–P(1)	174.64(17)	N(1)–C(17)–P(1)	114.9(4)
C(2)–Mo(1)–P(1)	87.54(17)	N(3)–C(37)–P(2)	117.3(3)
C(17)–P(1)–Mo(1)	123.14(18)		
Complex 7			
Pd(1)–P(2)	2.2523(16)	P(2)–C(33)	1.863(6)
Pd(1)–P(1)	2.2714(16)	Cl(1)–Pd(1A)	2.3916(16)
Pd(1)–Cl(1)	2.3606(16)	N(2)–C(13)	1.444(8)
P(1)–C(13)	1.846(6)	N(3)–C(33)	1.432(8)
P(2)–Pd(1)–P(1)	95.71(6)	C(33)–P(2)–Pd(1)	111.0(2)
P(2)–Pd(1)–Cl(1)	95.07(6)	Pd(1)–Cl(1)–Pd(1A)	97.29(6)
P(1)–Pd(1)–Cl(1)	167.98(6)	C(21)–N(2)–C(13)	118.9(5)
P(2)–Pd(1)–Cl(1A)	173.77(7)	C(25)–N(3)–C(33)	120.2(5)
P(1)–Pd(1)–Cl(1A)	87.09(6)	N(2)–C(13)–P(1)	117.1(4)
Cl(1)–Pd(1)–Cl(1A)	82.71(6)	N(3)–C(33)–P(2)	114.8(4)
C(13)–P(1)–Pd(1)	110.8(2)		
Complex ***8***			
Au(1)–P(1)	2.222(2)	P(1)–N(1)	1.683(7)
Au(1)–Cl(1)	2.293(3)	P(2)–N(3)	1.688(7)
P(1)–Au(1)–Cl(1)	177.54(10)	C(1)–N(1)–P(1)	120.9(5)
P(2)–Au(2)–Cl(2)	175.25(9)	C(5)–N(3)–P(2)	118.3(6)

3.13. X-ray structure determination

Single crystals of PNP1, **1**, **3** and **5** were grown from a mixture solvent of CH_2Cl_2/Et_2O, but those of **7** and **8** were obtained from solvent of $CH_2ClCH_2Cl/^iPr_2O$ and DMSO/acetone/Et_2O, respectively. Subsequent structure analysis showed that the crystals of **1**, **7** and **8** contained CH_2Cl_2, CH_2ClCH_2Cl and DMSO solvent molecules, respectively. The data collections were carried out at 293(2) K on a Bruker SMART 1000 CCD diffractometer using Mo Kα radiation (0.71073 Å). Data collection at 293 K and reduction were performed using the SMART and SAINT software with frames of 0.3° oscillations. An empirical absorption correction was applied using the SADABS program. An empirical absorption correction was applied using ψ-scan data. The structures were solved by direct methods and all non-hydrogen atoms were subjected to anisotropic refinement by full-matrix least squares on F^2 using the SHELXTL package. Non-hydrogen atoms were subjected to anisotropic refinement. All hydrogen atoms were generated geometrically (C–H bond lengths fixed at 0.95 Å), assigned appropriate isotropic thermal parameters and included in structure factor calculations. Details of the crystals, data collections, and structure refinements are summarized in Table 1.

4. Supplementary material

Crystallographic data for the structural analysis have been deposited with the Cambridge Crystallographic Data Centre, CCDC Nos. 243659–243663 and 244406 for compounds PNP1, **1**, **3**, **7**, **5** and **8**, respectively. Copies of this information may be obtained free of charge from The Director, CCDC, 12 Union Road, Cambridge CB2 1EZ, UK /(fax:+44 1223 336033; e-mail: deposit@ccdc.cam.ac.uk or www: http://www.ccdc.cam.ac.uk).

Acknowledgment

This work was supported by the National Science/ Foundation of China (Project Grant No. 20102003).

References

[1] (a) E.W. Ainscough, A.M. Brodie, A.K. Burrell, A. Derwahl, G.B. Jameson, S.K. Taylor, Polyhedron 23 (2004) 1159;
(b) H.-F. Lang, P.E. Fanwick, R.A. Walton, Inorg. Chim. Acta 329 (2002) 1;
(c) S.-M. Kuang, P.E. Fanwick, R.A. Walton, Inorg. Chem. 41 (2002) 405;
(d) S.J. Coles, S.E. Durran, M.B. Hursthouse, A.M.Z. Slawin, M.B. Smith, New J. Chem. 25 (2001) 416;
(e) M. Kranenburg, Y.E.M. van Burgt, P.C.J. Kamer, P.W.N.M. van Leeuwen, K. Goubitz, J. Fraanje, Organometallics 14 (1995) 3081;
(f) K. Hiraki, S. Khono, M. Onishi, T. Kuwahara, Y. Michita, Inorg. Chim. Acta 245 (1996) 243;
(g) Q.-S. Li, F.-B. Xu, D.-J. Cui, K. Yu, X.-S. Zeng, X.-B. Leng, H.-B. Song, Z.-Z. Zhang, Dalton Trans. (2003) 1551.
[2] B.D. Steffey, A. Miedaner, M.L. Maciejewski-Farmer, P.R. Bernatis, A.M. Herring, D.L. DuBois, Organometallics 13 (1994) 4844.

[3] C. Hahn, A. Vitagliano, F. Giordano, R. Taube, Organometallics 17 (1998) 2060.
[4] G.R. Newkome, D.C. Hager, J. Org. Chem. 43 (1978) 947.
[5] (a) Z.-Z. Zhang, H. Cheng, Coord. Chem. Rev. 147 (1996) 1, and references cited therein;
(b) H.-B. Song, Z.-Z. Zhang, T.C.W. Mak, Inorg. Chem. Commun. 5 (2002) 442, and references cited therein.
[6] (a) C. Hahn, M. Spiegler, E. Herdtweck, R. Taube, Eur. J. Inorg. Chem. (1999) 435;
(b) L. Barloy, S. Ramdeehul, J.A. Osborn, C. Carlotti, F. Taulelle, A. De Cian, J. Fischer, Eur. J. Inorg. Chem. (2000) 2523;
(c) G.-C. Jia, H.M. Lee, I.D. Williams, C.P. Lau, Y.Z. Chen, Organometallics 16 (1997) 3941;
(d) C. Hahn, J. Sieler, R. Taube, Polyhedron 17 (1998) 1183;
(e) L. Barloy, S.Y. Ku, J.A. Osborn, A. De Cian, J. Fischer, Polyhedron 16 (1997) 291;
(f) C. Hahn, A. Vitagliano, F. Giordano, R. Taube, Organometallics 17 (1998) 2060;
(g) N. Rahmouni, J.A. Osborn, A. De Cian, J. Fischer, A. Ezzamarty, Organometallics 17 (1998) 2470.
[7] (a) W. Schirmer, U. Florke, H.-J. Haupt, Z. Anorg. Allg. Chem. 545 (1987) 83;
(b) W. Schirmer, U. Florke, H.-J. Haupt, Z. Anorg. Allg. Chem. 574 (1989) 239.
[8] S.-M. Kuang, P.E. Fanwick, R.A. Walton, Inorg. Chim. Acta 338 (2002) 219.
[9] J. Andrieu, J.-M. Camus, J. Dietz, P. Richard, R. Poli, Inorg. Chem. 40 (2001) 1597.
[10] S.-M. Kuang, D.G. Cuttell, D.R. McMillin, P.E. Fanwick, R.A. Walton, Inorg. Chem. 41 (2002) 3313.
[11] S.-M. Kuang, P.E. Fanwick, R.A. Walton, Inorg. Chim. Acta 305 (2000) 102.
[12] L. Malatesta, L. Naldini, G. Simonetta, F. Cariati, Coord. Chem. Rev. 1 (1966) 255.
[13] K. Zhang, J. Prabhavathy, J.H.K. Yip, L.L. Koh, G.K. Tan, J.J. Vittal, J. Am. Chem. Soc. 125 (2003) 8452.